

# Optimization of the filling and solidification of large ingots

K. Marx, S. Rödl, S. Schramhauser, M. Seemann

*Ingot casting is an important process for the production of special steel products e.g. for power generation and automobile industry or offshore applications. These products must fulfill highest requirements concerning steel cleanliness and homogeneity. Concerning these requirements flow conditions and the course of solidification during the casting process are of essential importance. Against this background systematic investigations were performed concerning these phenomena by application of advanced physical and numerical simulation methods. In a physical model flow conditions during the filling process were investigated via flow visualization and laser-optical measuring systems. Important information concerning the time-dependent flow condition and quantitative information on flow velocities were obtained. Also numerical simulation with an enhanced CFD programme was performed in order to get further information on inclusion behavior with regard to inclusion separation, mould powder entrainment and solidification. The influence of the feeding system design, the filling rate as well as temperature conditions with a special view to the hot top design was assessed. Optimized constructive and process parameters were elaborated. The results prove the potential of developing a better controlled casting and solidification process by application of physical and numerical simulation methods.*

**Parole chiave:** Ingot casting - Mould filling - Solidification - Inclusion separation - Physical model trials - Numerical simulation

## INTRODUCTION

The physical phenomena in the ingot casting mould are difficult to observe and to measure. But also the physical and numerical modelling of the filling and solidification process is not easy to do. In spite of big advances in hardware and software development the simultaneous simulation of filling and solidification as well as behaviour of inclusions is not yet state of the art. Therefore the work described hereafter aimed at the further development of advanced numerical models for the computation of the filling and solidification process as well as the behaviour of inclusions. For the validation of the numerical simulation physical model trials with flow visualization and laser-optical measurements were performed. Hints for the optimization of the ingot casting process are given.

**Kersten Marx, Sigurd Rödl**

VDEh-Betriebsforschungsinstitut GmbH, Germany

**Sebastian Schramhauser, Martin Seemann**

Buderus Edelstahl GmbH, Germany

*Paper presented at the 2nd Int. Conf. Ingot Casting Rolling and Forging - ICRF 2014, Milan 7-9 May 2014*

## FURTHER DEVELOPMENT OF EXISTING NUMERICAL PROGRAMME

An existing numerical programme (based on Ansys/FLUENT) was developed for three dimensional simulations of multiphase fluid flow dynamics. The model development was focused on the following topics:

- Improved simulation of the unsteady filling and solidification process with the Volume of Fluid (VOF) method, modelling the movement of free surfaces.
- Simulation of inclusion behaviour/separation with consideration of agglomeration, separation and trapping.

**Numerical CFD tools.** The numerical programme used for the simulation of the multiphase flow is working according to the finite volume method. The fluids are assumed to be incompressible obeying the Navier-Stokes equations. Turbulence was simulated using RANS equations with standard k- $\epsilon$ -model. Moreover, the PRESTO discretization method was adopted to discretize the pressure. The PISO scheme was used to solve the pressure velocity coupling. Second order upwind schemes were applied to the momentum, turbulent kinetic energy, and turbulent dissipation rate. The "Geo-Reconstruct" spatial discretization was employed for the volume fraction to calculate the interfaces between the phases with VOF. Additionally the Courant number of VOF was set to 0.25 as default.

After the filling of the mould the flow is more and more dominated by natural convection. For the realistic simulation of this flow the density has to be defined temperature dependent. It turned out that the calculations are more stable if the density is defined according to the Boussinesq approximation. Piecewise linear definition of the density values depending on temperature resulted in rapid divergence of the calculations.

Three advanced numerical methods have been developed and implemented by BFI to simulate mould filling and solidification process including motion and agglomeration of non metallic inclusions:

- numerical model for the agglomeration of inclusions
- user defined function (UDF) to dampen the inclusion movement in the solidified shell
- UDF for the separation of particles at a free surface.

To compute the agglomeration of non-metallic inclusions a particle tracking method was used basing on the Euler-Lagrange approach. The fluid phase is treated as a continuum, while the dispersed phase is solved by tracking a large number of particles on their way through the computed flow field. The particle tracks are computed for each computational step and a possible collision partner is generated from the average values of particle properties and velocities of all particles in the flow cell.

The collision probability  $P_c$  obtained from the kinetic theory of gases depends on the collision frequency  $f_c$  and the time step size  $\Delta t$  and can be expressed by the properties of the two particles (tracked particle and collision partner) colliding. These properties are the particle diameters  $d_{p,t}$  and  $d_{p,c}$  and velocities  $\vec{u}_{p,t}$  and  $\vec{u}_{p,c}$  of the tracked particle and the collision partner. In Eq. 1  $n_p$  is the number of particles per unit volume. Collision probability is governed by the relative velocity between particles, the size of particles and the turbulence level of the flow.

$$P_c = f_c \Delta t = \frac{\pi}{4} (d_{p,t} + d_{p,c})^2 |\vec{u}_{p,t} - \vec{u}_{p,c}| n_p \Delta t \quad (1)$$

After determination of the collision probability this is compared to a random number from a uniform distribution in the interval [0,1]. If the collision probability is larger than this random number, collision takes place.

Usually, smaller particles adhere at larger so called collector particles. Particles are surrounded by a layer of fluid which develops as a consequence of the motion of the particle. This layer must be penetrated. The collision probability is fairly high when a particle travels within a small distance to the collector particle. In turbulent flows, due to the unsteady movement of particles even a larger distance to the collector particle satisfies collision conditions compared to laminar flow.

**Collision particle properties.** In each control volume a collision particle is assumed. The size, velocity vector and the turbulent fluctuation of the collision particle arises from all the particles passing through the cell at the time and this is done by averaging all particles of a particle class.

The velocity components of the collision partner are com-

posed of the local particle mean velocity and fluctuating components randomly sampled from a probability distribution assumed to be Gaussian. Therefore only the local mean and root-mean-square (RMS) values of the velocity components are used. Each fluctuating component of the particle velocity is derived from the fluctuation of the fluid depending on a modified Stokes number, relating particle relaxation time to a characteristic time scale of the flow. The characteristic time scale in this Stokes number for turbulent flows is the turbulent integral time scale  $T_t$ . In the collision model  $T_t$  is determined by the following equation:

$$T_t = c_T \frac{2k}{3\varepsilon} \quad \text{with } c_T = 0.4 \quad (2)$$

Here  $k$  is the turbulent kinetic energy,  $\varepsilon$  is the turbulent energy dissipation and  $c_T$  is a constant.

**Post collision properties.** When modelling inter-particle collisions stochastically, without tracking every particle but defining a collision partner from the average of the particles in a control volume, the collision position has to be determined. Therefore a coordinate system is adjusted with the movement of the collision partner. A collision cylinder is aligned to that coordinate system and by two random numbers for the two angles perpendicular to the particle motion the collision point is fixed. If the particles do not agglomerate the velocity components after rebound are obtained by solving the momentum equation in connection to Coulomb's law of friction.

To model the behaviour of inclusion in the solidified part and in the transition area the mushy zone the drag force acting on the inclusion was adapted according to [1]. With the help of a User-defined-Function (UDF) the drag force is intensified depending on the liquid fraction in order to prevent a relative movement of the inclusions in the solidified shell.

The simulation focuses mainly on the remaining inclusions in the melt, rather than the trapped inclusions. Since the trapped inclusions will never return back to the melt region, they can be treated as escaped from the melt. Because these inclusions are not of interest, they can be deleted from the computational domain in the simulation model.

The position, where the inclusions can be deleted, should be defined mathematically. This can be done by the coupling with the VOF model. In the VOF model, each numerical grid cell contains a local value  $F$ . It denotes the liquid fraction in the cell. That means for a liquid/air two-phase model:

- $F = 1$ : the cell is filled with liquid phase only
- $F = 0$ : the cell is filled with air only
- $0 < F < 1$ : the cell is located at the interface between liquid and air.

The inclusions located in a cell with a value  $F < 0.1$ , where defined as trapped at the interface, and can therefore be deleted from the computational domain.

The implementation of this modification was carried out with a UDF in the FLUENT package. A macro was employed to update the value of  $F$  for the individual particle positions in every time step.

## INVESTIGATION OF MOULD FILLING AND INGOT SOLIDIFICATION

The calculations and model trials were done for a teeming rate of 3.3 t/min in the mould and 1.1 t/min in the hot top. A first assumption for the inclusions size distribution was derived from the distribution given by Zhang et al. [2], neglecting the particles greater than 200 µm. A convenient representation of the inclusion size distribution is the Rosin-Rammler expression. The Rosin-Rammler distribution function is based on the assumption that an exponential relationship exists between inclusion diameter  $d$  and the mass fraction  $Y_d$  of inclusion with diameter greater than  $d$ . The complete range of sizes is divided into an adequate number of discrete intervals; each represented by a mean diameter for which trajectory calculations are performed. If the size distribution is of the Rosin-Rammler type, the mass fraction  $Y_d$  of inclusions of diameter greater than  $d$  is given by:

$$Y_d = e^{-x} \quad x = (d/d^*)^n$$

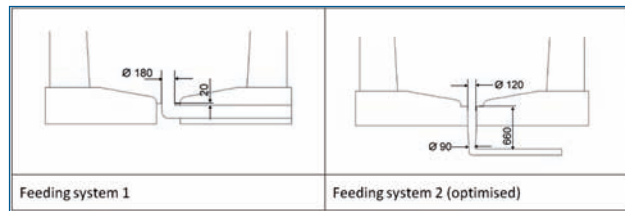
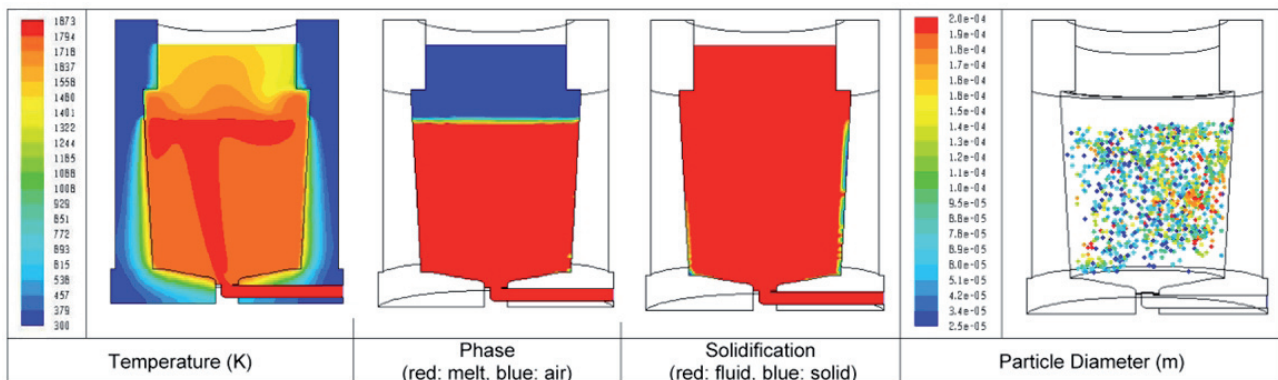


**Fig. 1 - Geometry of the selected feeding systems**

*Fig. 1 - Geometria del sistema di alimentazione selezionato*

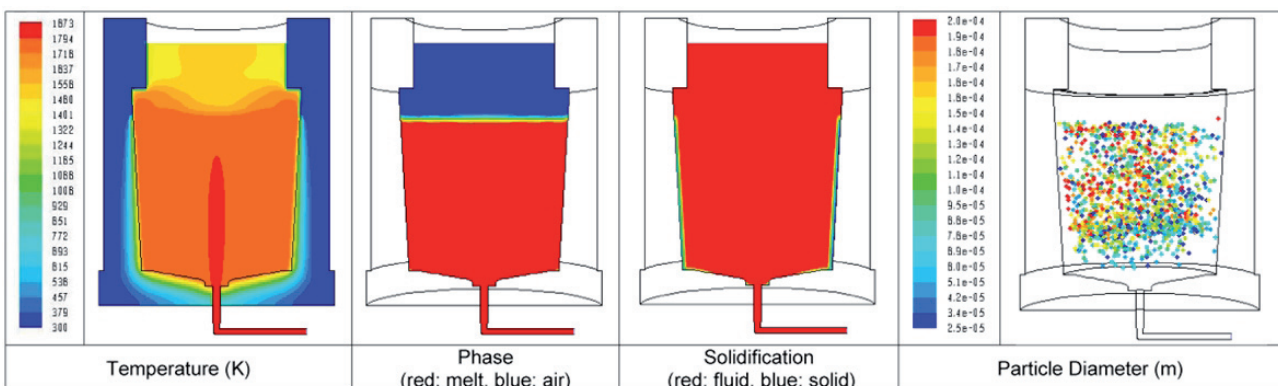
where  $d^*$  is the size constant (mean diameter) and  $n$  is the size distribution parameter (spread). For the chosen distribution the determined values are:  $d^* = 130 \mu\text{m}$  and  $n = 1.1$ . Two feeding system geometries for a mould (100 t ingot) were selected for the investigation. Fig. 1 shows the chosen geometries.

Fig. 2 shows the calculated temperature field, the phase distribution, the beginning of the solidification and the particle distribution 20 min after start of filling for feeding



**Fig. 2 - Calculated temperature field, phase distribution, solidifying shell and particle distribution 20 min after start of filling for feeding system 1**

*Fig. 2 - Campo di temperatura calcolata, distribuzione di fase, guscio di solidificazione e distribuzione delle inclusioni 20 min dopo l'inizio del riempimento per il sistema di alimentazione 1*



**Fig. 3 - Calculated temperature field, phase distribution, solidifying shell and particle distribution 20 min after start of filling for feeding system 2**

*Fig. 3 - Campo della temperatura calcolata, distribuzione di fase, guscio di solidificazione e distribuzione delle inclusioni 20 min dopo l'inizio del riempimento per il sistema di alimentazione 2*

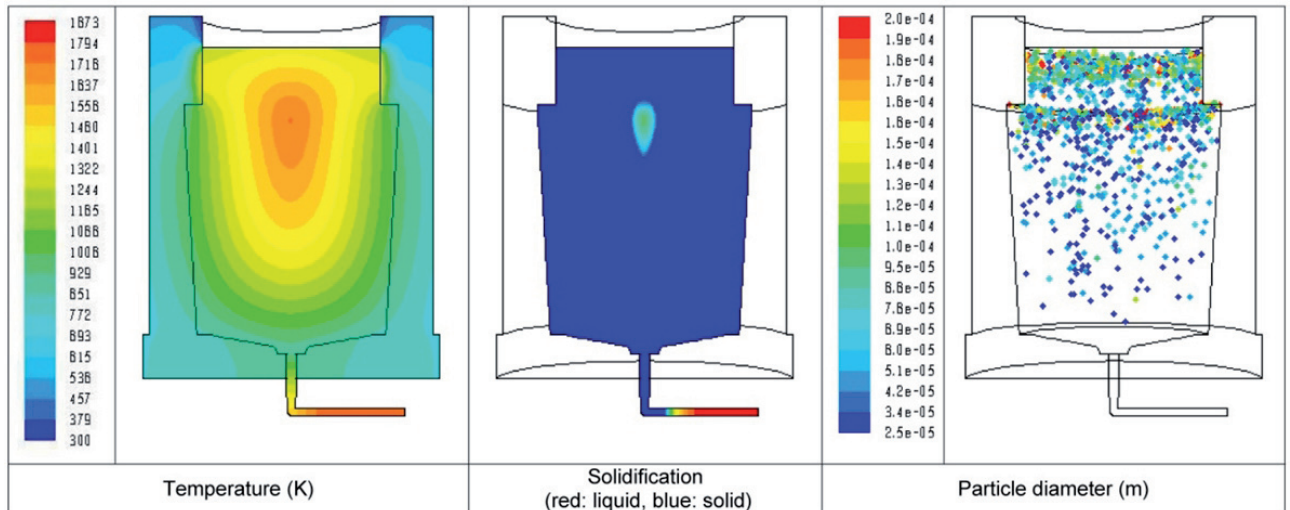


**Fig. 4 - Calculated temperature field, solidifying shell and particle distribution 17 h after start of filling for feeding system 2**

*Fig. 4 - Campo della temperatura calcolata, guscio di solidificazione e distribuzione delle inclusioni 17 min dopo l'inizio del riempimento per il sistema di alimentazione 2*

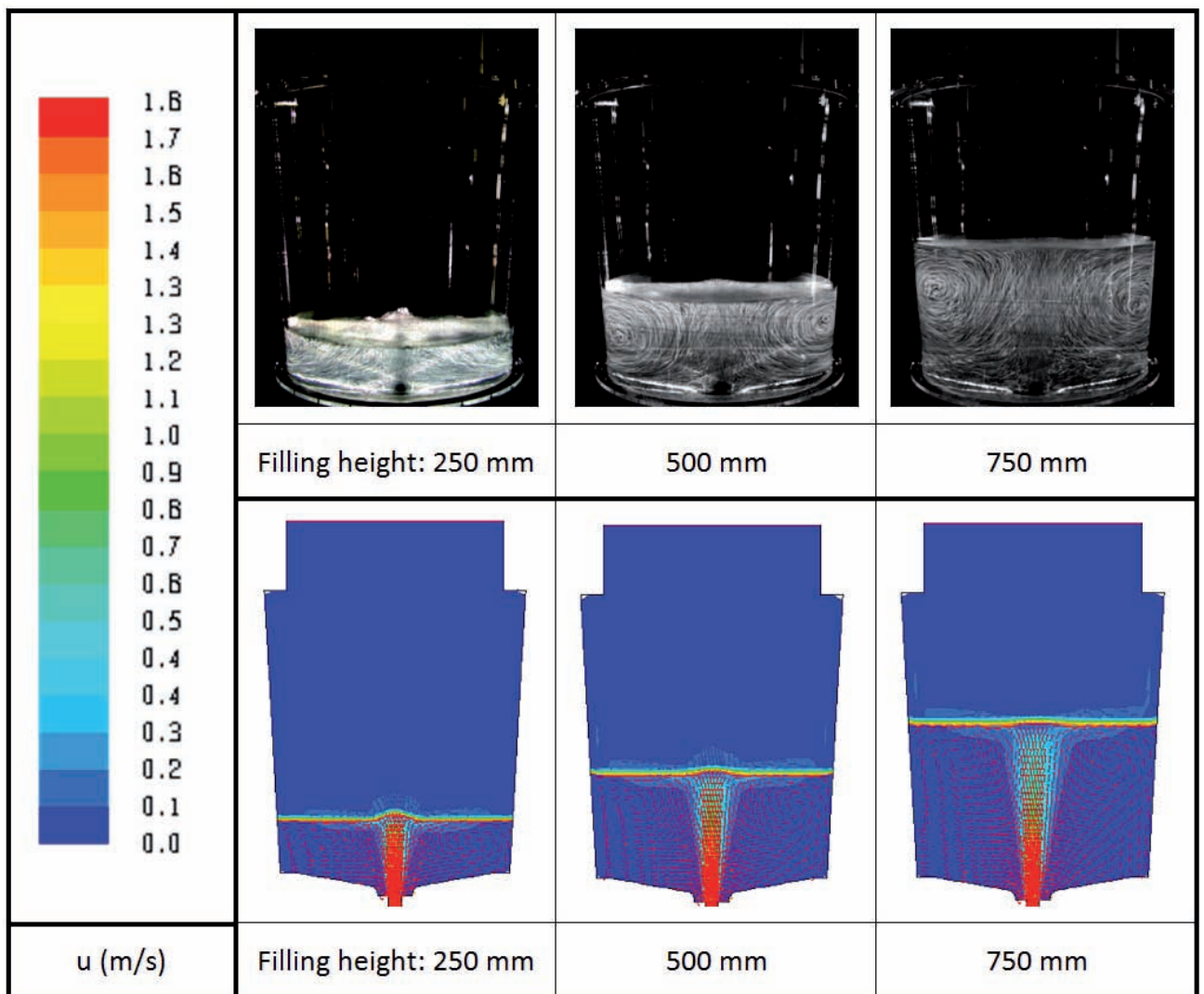


**Fig. 5 - Visualized and calculated flow field in the physical model for filling heights up to 750 mm**

*Fig. 5 - Campo di flusso visualizzato e calcolato nel modello fisico per altezze di riempimento fino a 750 mm*

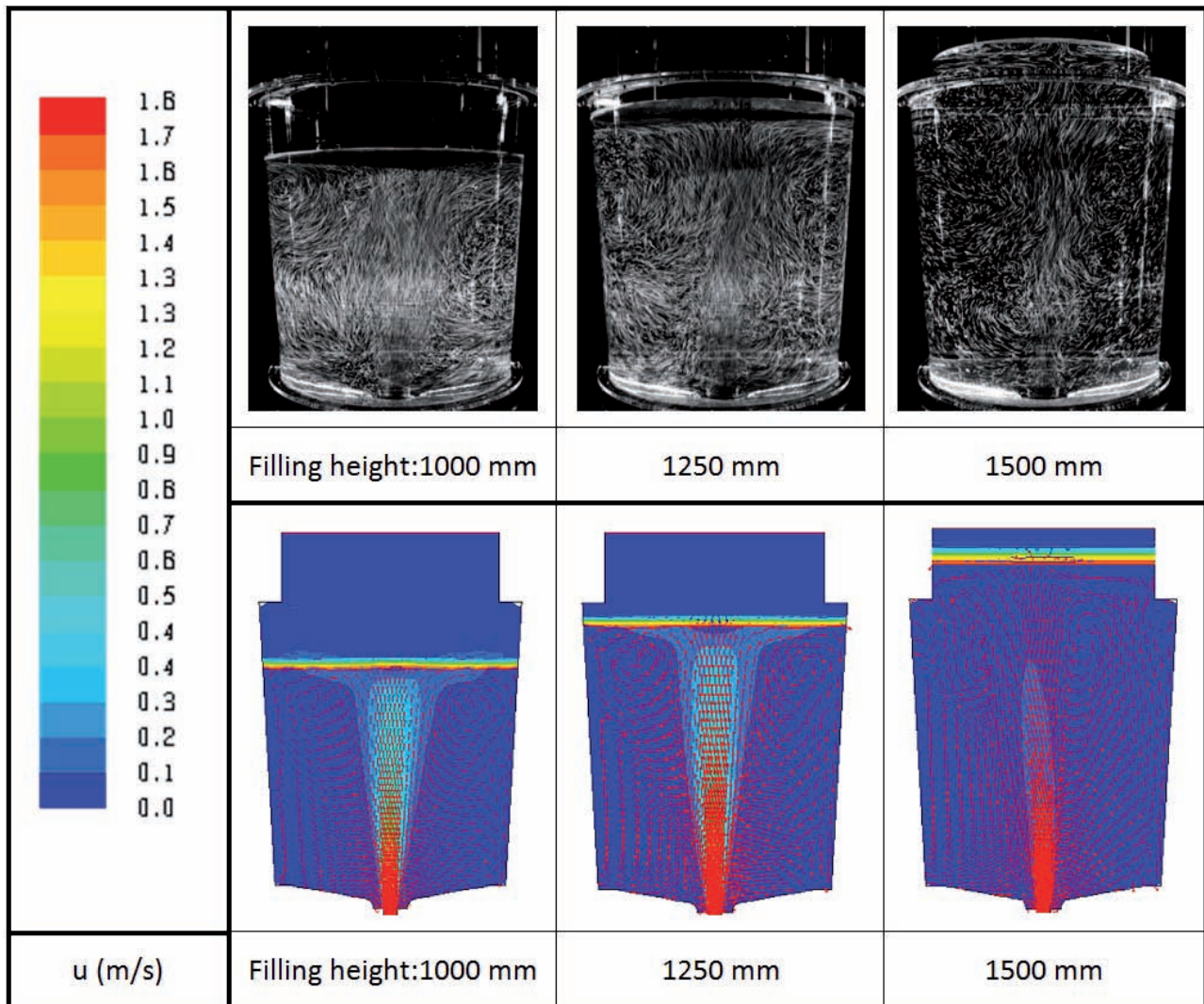


**Fig. 6 - Visualized and calculated flow field in the physical model for filling heights from 1000 mm up to 1500 mm**

*Fig. 6 - Campo di flusso visualizzato e calcolato nel modello fisico per altezze di riempimento da 1000 mm fino a 1500 mm*

system 1. Because the filling jet is not exactly vertical, the initial solidification is asymmetric. Even the big particles do not float to the surface because of a strong flow downwards on the right hand side. This is detrimental for the separation of inclusions.

For the optimized feeding system the inlet jet and the solidified shell are symmetric and the big particles start to float to the surface, s. Fig. 3. So a better separation of inclusions can be expected.

Fig. 4 shows the calculated temperature field, the solidification and particle distribution 17 hours after start of filling. The final solidification occurs not completely in the region of the hot top and a lot of particles are not separated at the melt surface.

A physical model of the Buderus 100 t-ingot-mould with the optimised feeding system was designed in the scale 1 : 2.

Physical model trials are often subject to limitations due to the specific circumstances in operational plants. In steel production large dimensions, thermal conditions and real

fluid properties often restrict laboratory work. Realistic conditions can be approximated using similarity theory. With the aid of dimensionless numbers model conditions can be adjusted to obtain appropriate results.

For physical modelling of fluid dynamic processes, following relevant dimensionless numbers have to be taken into account. For isothermal modelling of single-phase melt flow, these are the Reynolds ( $Re$ ) and the Froude number ( $Fr$ ):

$$Re = \frac{\text{inertial forces}}{\text{viscous forces}} = \frac{u \cdot \rho \cdot l}{\mu} = \frac{u \cdot l}{\nu} \quad (3)$$

$$Fr = \frac{\text{inertial forces}}{\text{body forces}} = \frac{u^2}{g \cdot l} \quad (4)$$

Here  $u$  represents the flow velocity,  $\rho$  the density,  $\mu$  the dynamic viscosity,  $\nu$  the kinematic viscosity,  $l$  a characteristic length and  $g$  the gravitational acceleration.

Another dimensionless number for similarity of flow is the Weber number ( $We$ ). This number describes the ratio

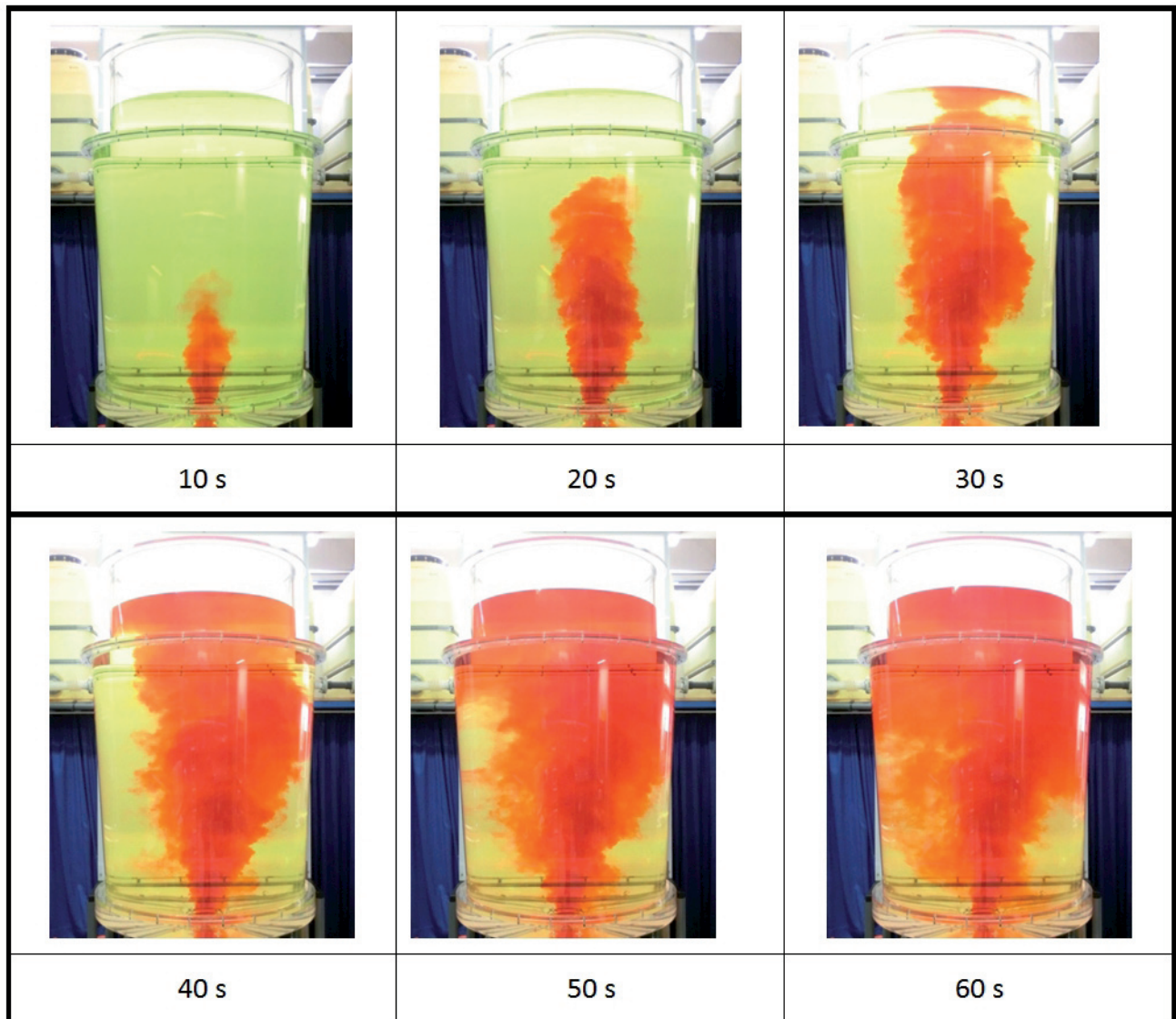


**Fig. 7 - Visualized flow in the physical model of the Buderus mould (dye injection)**

*Fig. 7 - Flusso visualizzato nel modello fisico dello stampo Buderus (stampo ad iniezione)*

between inertial force to the surface tension  $\sigma$  and reads:

$$We = \frac{\text{inertial forces}}{\text{surface tension}} = \frac{u^2 \cdot \rho \cdot l}{\sigma} \quad (5)$$

When similarity of flow is approximated with respect to  $Re$  and  $Fr$  the Weber number differs for air-water and liquid steel-liquid mould powder system respectively. This has to be considered when phenomena regarding free surfaces are discussed.

The trials for validating the calculated flow field were done for equal Reynolds number in order to have similar turbulence conditions. The flow in the model was visualized in a light section through the symmetry plane with particles which follow the flow. Fig. 5 and Fig. 6 show the visualized and the calculated flow field for different filling heights in comparison.

The visualized and calculated flow patterns are very similar. The flow in the physical model of the Buderus 100 t-ingot-mould with the optimized feeding system was also visualized by dye injection, s. Fig. 7. The flow is symmetric and shows good mixing.

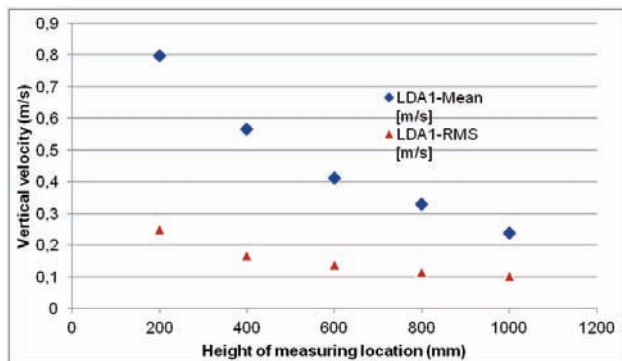
Measurements with Laser Doppler Anemometry were per-

formed in the symmetry axis of the physical model. With the optimized feeding system a symmetric flow is achieved. The vertical component of the velocity and the RMS value (Root mean square of the velocity fluctuation) is decreasing with the height of the filling level, so that the risk of mould powder entrapment is decreasing with filling time, s. Fig. 8.

#### OPTIMIZATION OF HOT TOP

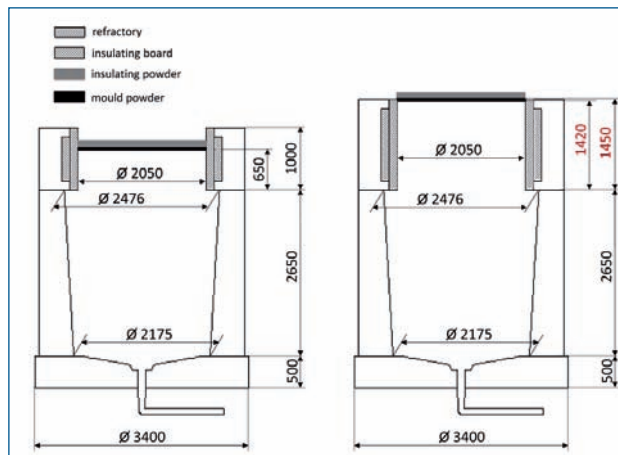
In order to determine the influence of the hot top height on the inclusion separation a hot top with increased height was studied. Fig. 9 shows the original hot top and the modified one in comparison.

Fig. 10 shows the calculated temperature field, solidification front and particle positions in the mould with hot top 2, 24 hours after end of filling. The results of the CFD simulation show that the temperature values in the hot top are still high after 24 hours. The final solidification now takes place in the



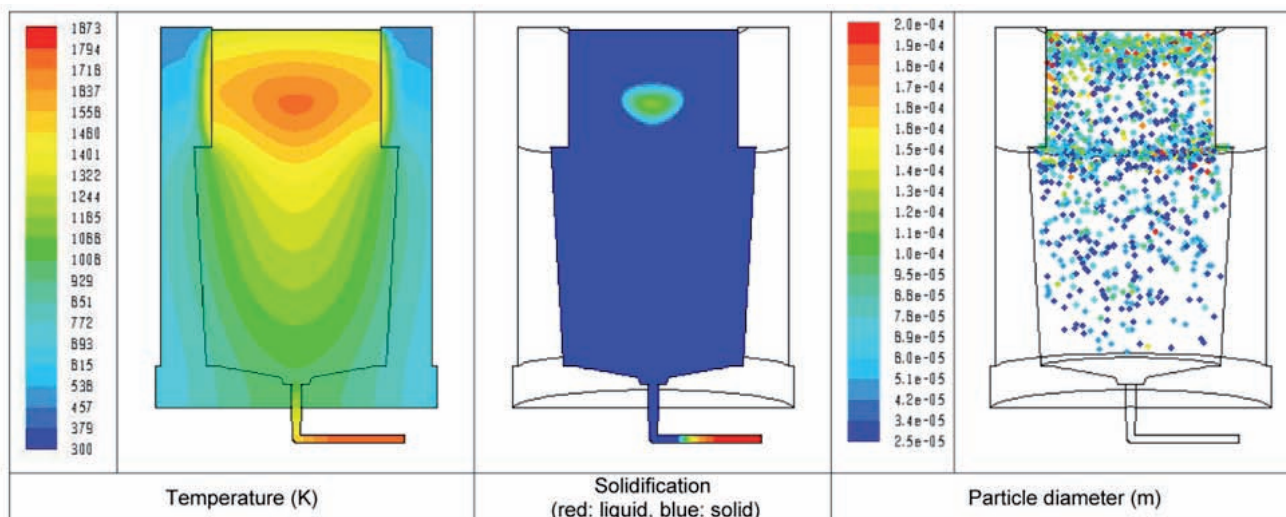
**Fig. 8 - Mean vertical velocity component and RMS value measured in the symmetry axis of the physical model of the Buderus mould with optimized feeding system**

Fig. 8 - Componente di velocità verticale media e valore RMS misurati sull'asse di simmetria del modello fisico dello stampo Buderus con sistema di alimentazione ottimizzato



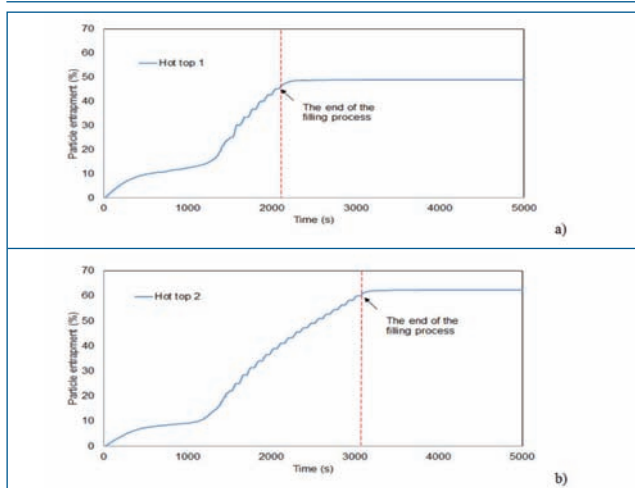
**Fig. 9 - Geometry of original (left) and modified hot top (right) in comparison**

Fig. 9 - Confronto fra geometria della zona alta calda della lingottiera originale (destra) e modificata (sinistra)



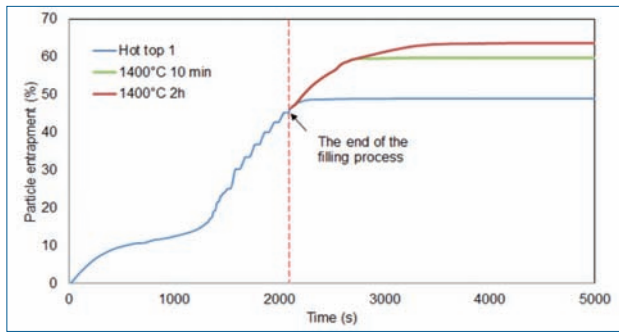
**Fig. 10 - Calculated temperature field, solidification front and particle positions in the mould with hot top 2, 24 hours after the end of filling**

Fig. 10 - Campo della temperatura calcolata, fronte di solidificazione e posizione delle inclusioni all'interno della lingottiera con zona alta calda 2, 24 ore dopo la fine del riempimento



**Fig. 11 - Calculated percentage of the trapped inclusions in the ingot for original (a) and increased hot top height (b)**

Fig. 11 - Percentuale calcolata delle inclusioni presenti nel lingotto nel caso della misura originale della zona alta calda (a) e in quello della sua misura aumentata (b)



**Fig.12 - Calculated percentage of the trapped inclusions in the ingot for original practice (blue), the application of exothermic mould powder (green) and additional heating of the melt surface for 2 hours (red)**

*Fig. 12 - Percentuale calcolata delle inclusioni presenti nel lingotto nel caso del procedimento originale (blu), dell'applicazione della polvere esotermica (verde) e dell'ulteriore riscaldamento di 2 ore della superficie fusa (rosso)*

hot top region. The inclusions have more time to separate, because of the longer filling and solidification process. Fig. 11 shows that the percentage of inclusions entrapped in the slag can be increased with a higher hot top height.

## CONCLUSIONS

Advanced numerical models for the computation of the filling and solidification process as well as the behaviour of inclusions were further developed. User defined functions for agglomeration and the trapping of inclusions at the free surface were implemented. Numerical simulations for two feeding systems and hot top geometries for an actual mould design were performed. A physical model was built for the selected mould. Flow visualization trials and laser-optical measurements were performed. The results were compared with the results of the numerical simulation. The positive influence of increased hot top height, adjusted feeding rate and temperature control of the hot top on solidification and inclusion separation was determined.

## ACKNOWLEDGEMENT

The research leading to these results has received funding from the European Union's Research Fund for Coal and Steel (RFCS) research programme under grant agreement n° RFSR-CT-2011-00006). The authors want to thank for the financial support.

List of symbols		
c	constant	–
d	diameter	m
d*	size constant (mean diameter)	m
f	frequency	1/s
Fr	Froude number	-
F	liquid fraction in cell	-
g	gravitational acceleration	m/s <sup>2</sup>
k	turbulent kinetic energy	m <sup>2</sup> /s <sup>2</sup>
l	characteristic length	m
n	size distribution parameter (spread)	-
p	probability of collision	-
Re	Reynolds number	-
t	time scale	s
u	velocity	m/s
We	Weber number	-
x	exponent	-
Y	mass fraction	-
Greek Symbols		
ε	turbulent dissipation	m <sup>2</sup> /s <sup>3</sup>
ρ	density	kg/m <sup>3</sup>
μ	dynamic viscosity	Ns/m <sup>2</sup>
ν	kinematic viscosity	m <sup>2</sup> /s
σ	surface tension	N/m
Indices		
c	collision, collector	
d	diameter	
f	frequency	
p	particle	
t	tracked, turbulent velocity	
T	time scale	

## REFERENCES

- [1] C. Tscheuschner, R. Koitzsch and S. Rödl, Application of enhanced simulation approaches for investigation of multiphase phenomena in the mould, Proceedings of the 4th European Conference on Modelling and Simulation of Metallurgical Processes in Steelmaking, Düsseldorf, July 28-30, 2011, (CD-ROM)
- [2] L. Zhang, B. Rietow, B.G. Thomas and K. Eakin, Large inclusions in plain-carbon steel ingots by bottom teeming. ISIJ International, Vol. 46 (2006), No. 5, pp. 670-679

## Ottimizzazione del riempimento e solidificazione di lingotti di grandi dimensioni

**Parole chiave:** Colata in lingottiera - Processi - Solidificazione - Modellazione - Simulazione numerica

La colata in lingottiera è un importante processo per la fabbricazione di prodotti in acciaio speciale utilizzati ad esempio nell'industria per la produzione di energia e in quella automobilistica o in applicazioni offshore. Questi prodotti devono soddisfare i più stringenti requisiti di purezza e omogeneità dell'acciaio. Per quanto riguarda questi requisiti, assumono fondamentale importanza le condizioni di flusso e il processo di solidificazione durante l'operazione di colata.

In questo contesto sono state eseguite indagini sistematiche di questi fenomeni mediante applicazione di metodi avanzati di simulazione fisica e numerica. In un modello fisico sono state esaminate le condizioni di flusso durante il processo di riempimento mediante visualizzazione del flusso e sistemi di misurazione e laser ottici. Sono state così ottenute importanti informazioni sulla condizione di flusso dipendente dal tempo e informazioni quantitative sulle velocità di flusso. Inoltre è stata eseguita la simulazione numerica mediante programma avanzato CFD al fine di ottenere ulteriori informazioni sul comportamento delle inclusioni e in particolare sulla separazione delle inclusioni, trascinamento delle polveri in lingottiera e solidificazione.

Sono stati valutate l'influenza del sistema di alimentazione, la velocità di riempimento e le condizioni di temperatura con particolare riguardo al tipo di progetto della parte alta calda. Sono stati elaborati parametri costruttivi e di processo ottimizzati. I risultati ottenuti dimostrano le potenzialità di sviluppo di un processo di colata e solidificazione più controllato mediante l'applicazione di metodi di simulazione fisici e numerici.